International Journal of Applied Power Engineering (IJAPE)
Vol. 15, No. 1, March 2026, pp. 238~247
ISSN: 2252-8792, DOI: 10.11591/ijape.v15.i1.pp238-247

Artificial neural network-optimized bridgeless Landsman converter for enhanced power factor correction in electric vehicle applications

Podila Purna Chandra Rao[1,2], Radhakrishnan Anandhakumar[1], T. Vijay Muni[3], L. Shanmukha Rao[4]
[1]Department of Electrical Engineering, Faculty of Engineering and Technology, Annamalai University, Chidambaram, India
[2]Department of Electrical and Electronics Engineering, Sasi Institute of Technology and Engineering, Tadepalligudem, India
[3]Department of Electrical and Electronics Engineering, Koneru Lakshmaiah Education Foundation, Vaddeswaram, India
[4]Department of Electrical and Electronics Engineering, Kallam Haranadhareddy Institute of Technology, Dasaripalem, India

Article Info

Article history:

Received Mar 31, 2025
Revised Nov 13, 2025
Accepted Nov 28, 2025

Keywords:

Artificial neural network
Bridgeless Landsman converter
Hysteresis controller
PI controller
Power quality improvement
Pulse width modulation

ABSTRACT

Electric vehicles (EVs) are gaining popularity globally due to their energy-efficient battery storage systems, low carbon emissions, and eco-friendly operation. By transforming both the transportation and electrical sectors, EVs could create a synergistic relationship that reduces fossil fuel use and improves renewable energy integration. However, this convergence emphasizes the necessity for appropriate power factor correction (PFC) methods, especially in EV battery charging systems, to alleviate supply-end PQ concerns. Use of a bridgeless Landsman converter (BLC), noted for its efficiency and link voltage monitoring, is innovative in this research. A proportional-integral (PI) controller tuned by an artificial neural network (ANN) improves prediction and classification, especially response time. The ANN-based PI controller optimises system performance in real time using adaptive control. Using a hysteresis controller attached to a pulse width modulation (PWM) generator regulates the converter's steady-state switching frequency for accurate and consistent output. The proposed approach reduces harmonic distortions and improves operating efficiency. This comprehensive architecture improves power factor and addresses significant PQ concerns in EV charging infrastructure. Integrating improved control tactics and converter design shows that this approach may support electric car technology developments. MATLAB simulations show that power factor correction (PFC) charges EV batteries quickly and effectively. Findings suggest the technique could increase power quality, system efficiency, and EV uptake.

Corresponding Author:

Podila Purna Chandra Rao
Department of Electrical Engineering, Faculty of Engineering and Technology, Annamalai University
Chidambaram, India
Email: purnachandrarao.phd@gmail.com

1. INTRODUCTION

Electric vehicles (EVs) play a pivotal role in fostering sustainable and efficient transportation by addressing global challenges such as global warming, rising emissions, dwindling fossil fuel reserves, and surging fuel prices [1]. By integrating renewable energy-based power generation and EV technology, these vehicles present a promising solution to these pressing issues. As a viable and sustainable mode of transportation, EVs have garnered significant attention due to their alignment with the goals of reducing carbon footprints and advancing battery technology [2].

The quality of input and output power in EV systems is managed through power factor correction (PFC) techniques. However, conventional PFC methods are hindered by power losses and inadequate handling of large load transients [3]. These limitations can be effectively addressed by integrating PFC techniques with advanced converter systems [4].

Traditional boost converters, while offering high boosting ratios in ideal conditions, are often impractical due to voltage stress and dynamic instability [5]. These challenges necessitate higher-rated switches for reliable operation [6]. Buck-boost converters overcome some limitations by supporting both voltage bucking and boosting, but their discontinuous input current restricts their usability [6], [7]. The Cuk converter improves voltage gain with reduced switching losses and enhanced voltage regulation; however, its static gain is inadequate for low-voltage PV systems, and its inverted output limits its application [8], [9]. Similarly, the single-ended primary-inductor converter (SEPIC) converter offers high gain and a non-inverted output, yet its performance is impeded by significant current ripples, making it unsuitable for high-power interleaved EV chargers [10]-[15].

The Landsman converter, a derivative of the SEPIC and Cuk converters, offers better voltage conversion ratios while maintaining continuous input and output currents, which is ideal for EV battery charging where voltage stability and low current ripple are critical [16]. Though the Landsman converter is a fourth-order nonlinear system, this complexity is advantageous when using artificial neural networks (ANNs) [17]. ANNs can learn and adapt to complex dynamics more effectively than traditional control methods, thus making the higher-order dynamics manageable and optimizable. While 2nd or 3rd order converters are simpler and may have lower switching losses, they lack the flexibility and performance range that the Landsman converter offers under dynamic input/output conditions typical in EV environments [18]-[20]. Its operation is optimized using a closed-loop proportional-integral (PI) controller, which ensures output stability by managing the on-off switching times and improving both static and dynamic system characteristics [21], [22]. The integration of ANNs augments the system's predictive capabilities, leveraging human intelligence to enhance detection and classification efficiency [23].

In this research, a bridgeless Landsman converter is implemented to achieve effective and noiseless operation. The converter's performance is regulated by an ANN-based PI controller, which aids in operational detection and classification. Additionally, a hysteresis controller coupled with a pulse width modulation (PWM) circuit ensures precise switching frequency regulation, leading to enhanced efficiency and reduced power quality issues. This framework underscores the potential of advanced converter and control strategies to address critical challenges in EV charging systems.

2. METHOD

This paper introduces a novel charging technique with improved PFC tailored for battery-operated electric vehicles (BEVs). The proposed method employs a bridgeless Landsman converter designed to minimize losses, enhance efficiency, and achieve higher voltage gain. The integration of an ANN-based PI controller facilitates effective converter control and ensures the transfer of maximum power [24]. Additionally, the controller aids in power detection and operational classification [25]. To predict steady-state switching frequencies and ensure reliable output generation, a hysteresis-regulated PWM generator is utilized. The basic schematic diagram of the proposed methodology is presented in Figure 1.

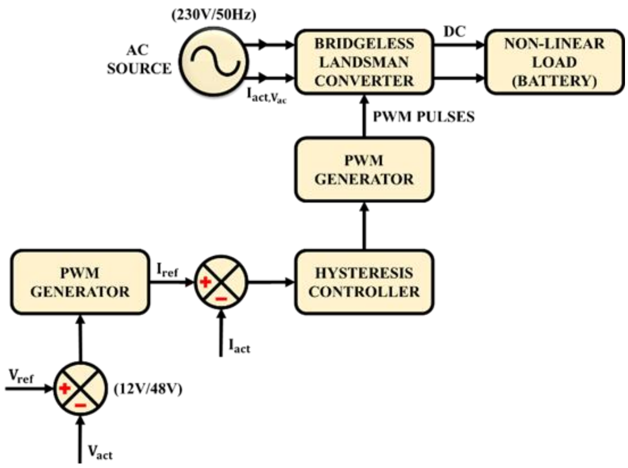

Figure 1. ANN based bridgeless Landsman converter for PFC

The proposed ANN based controllers compare the converter's voltage to a reference voltage and process it. A reference current is output by the controller and compared to the converter's current [26]. The hysteresis controller receives this comparison result. The Landsman converter's operation is regulated by the hysteresis controller's output, assuring steady voltage.

2.1. Bridgeless Landsman converter

The suggested method supplies AC mains power to the bridgeless Landsman converter at UPF. The converter has three modes. The voltages across switches S_1 and S_2 are denoted as V_{s1} and V_{s2}, respectively. The currents through inductors L_{I1} and L_{I2} are represented as I_{LI1} and I_{LI2}, while the currents through the output inductors L_{O1} and L_{O2} are denoted as I_{LO1} and I_{LO2}, respectively. Figure 2 illustrates the circuit diagram of the bridgeless Landsman converter.

- Mode 1: In this mode, switch S_1 is turned ON, causing capacitor C_1 to discharge and transfer its energy to charge inductor L_{I1}. During mode 1, inductor L_{O1} discharges, contributing to an increase in V_{DC} and I_{LI1}, while the voltage across capacitor C_1 decreases. Figure 3 shows the bridgeless Landsman converter circuit in mode 1.
- Mode 2: In this mode, both switches are in the OFF state, allowing the charging of inductor L_{O1} and capacitor C_1 to occur. Additionally, during mode 2, the input inductor L_{I1} discharges, resulting in a rise in the voltage across capacitor C_1. Figure 4 depicts the circuit configuration of the bridgeless Landsman converter during mode 2 of operation.
- Mode 3: In mode 3, discontinuous conduction causes inductor current discontinuity. The current ILI1 drops to zero when the inductor LI1 discharges fully. In the meantime, capacitor C1's voltage drops and the output inductor's current rises. Figure 5 shows the bridgeless Landsman converter circuit in mode 3.

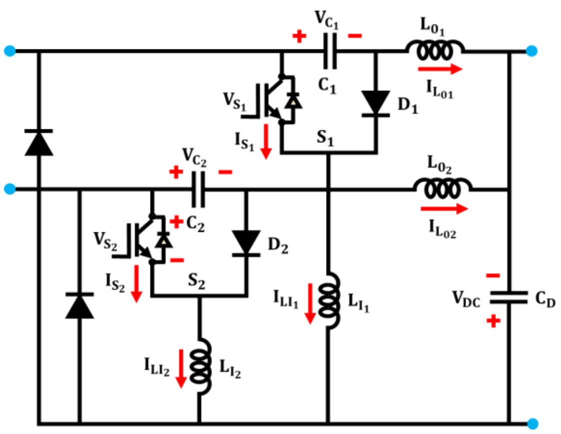

Figure 2. Circuit diagram of Landsman converter

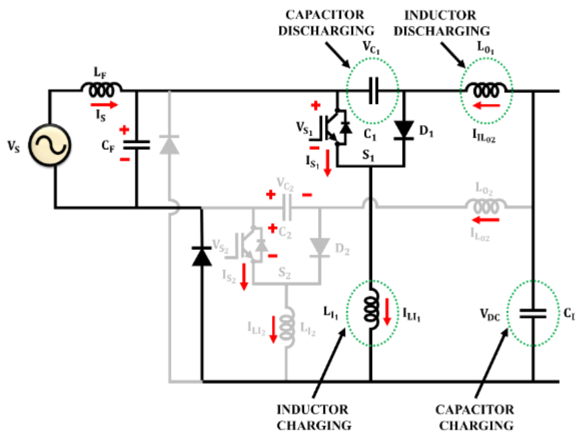

Figure 3. Converter operation in mode 1

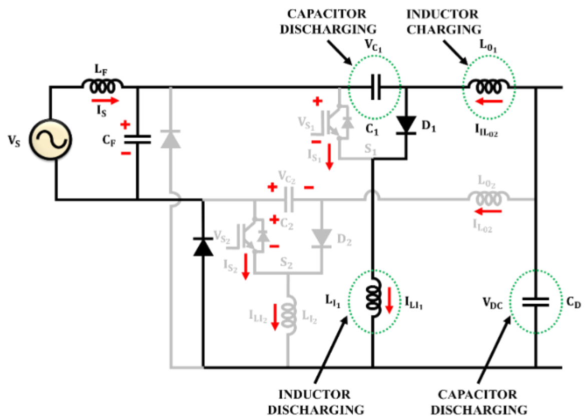

Figure 4. Converter operation in mode 2

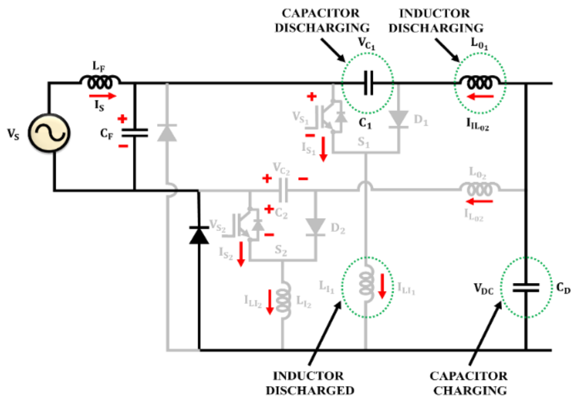

Figure 5. Converter operation in mode 3

The bridgeless Landsman converter's input voltage is as (1). Here, a maximum supply voltage as V_m and frequency is specified by f_L.

$$V_S(t) = V_m sin(\omega_L t) \\ = V_m \sin(2\pi f_L t) \quad (1)$$

$$V_{in} = \frac{2\sqrt{2}}{\pi} V_S \quad (2)$$

The duty cycle of the converter is calculated as (3).

$$D = \frac{V_{DC}}{V_{in}+V_{DC}} = \frac{V_{DC}}{|V_m \sin(\omega t)|+V_{DC}} \quad (3)$$

The value of inductors L_{O1} and L_{O2} is given as (4) and (5).

$$L_{O1} = L_{O2} = \left(\frac{V_S^2}{P_i}\right)\frac{D}{\Delta i f_S} = \frac{i}{\Delta i f_S}\left(\frac{V_S^2}{P_i}\right)\left(\frac{V_{DC}}{V_{in}+V_{DC}}\right) \quad (4)$$

$$= \frac{i}{\Delta i f_S}\left(\frac{V_{Smin}^2}{P_{max}}\right)\left(\frac{V_{DCmax}}{\sqrt{2}V_{smin}+V_{DC}}\right) \quad (5)$$

The value of inductors L_{IC1} and L_{IC2} is as (6).

$$L_{IC1} = L_{IC2} = \left(\frac{V_{Smin}^2}{P_{max}}\right)\frac{V_{DCmax}}{2\sqrt{2}V_{smin}f_S}\left(\frac{V_{DCmax}}{\sqrt{2}V_{smin}+V_{DCmax}}\right) \quad (6)$$

The value of capacitance C_1 and C_2 is given as (7).

$$C_1, C_2 = \frac{V_{DC}}{\kappa\{V_{DC}+V_{in}\}f_S(V_{DC}{}^2/P_i)}\left(\frac{V_{DC}}{V_{in}+V_{DC}}\right) \quad (7)$$

The value of capacitance C_D is given as (8).

$$C_D = \frac{P_{min}}{2\omega\Delta V_{DCmin}^2} \quad (8)$$

Bridgeless Landsman converters keep the PF near unity, assuring system stability.

2.2. ANN based PI controller

The introduction of an artificial neural network (ANN) effectively addresses the challenges of non-linear systems, enabling the generation of essential switching signals for the bridgeless Landsman converter. Its self-adaptive nature makes it highly suitable for managing uncertainties, parameter variations, and nonlinearities. ANN is typically utilized for system identification due to its learning and generalization capabilities. In this setup, the reference current required for the operation of the hysteresis controller is generated by the ANN-based PI controller. Figure 6 illustrates the structure of the ANN-based PI controller, where the state generator is provided with a voltage input.

$$V = \left[V_{DC,LOW}^{ref} \quad V_{DC,LOW}\right]^T \quad (9)$$

State x1 and x2 from the generator are in (10).

$$x_1 = V_e(m), x_2 = \frac{\delta x_1}{\delta m} \quad (10)$$

Equation for output error is calculated as (11).

$$Z(m) = V_o(m) - V_o(m-1) \quad (11)$$

Controlling signals are created by neuron cells in linked groups.

$$V(m) = V(m-1) + \sum_{k=i}^{ii} W_k\,(m) a_k(m) \tag{12}$$

System weight is W_k. Hebb's rule updates the neuron's weight, which is in (13).

$$\Delta W_k(m) = F_k(Y(m), a_{k(m)}) \tag{13}$$

For m^{th} moment, the change in weight is given as (14).

$$\Delta W_k(m) = -c\,\frac{\delta F_k(m)}{\delta W_k(m)} \tag{14}$$

Optimization tunes PI controller settings of $W_k(m)$.

$$I_S < \frac{C_{DC} V_{DC,LOW}^{ref}}{3K_p L_f} \tag{15}$$

$$I_S \leq \frac{V_S K_p}{2R_f K_p + L_f K_i} \tag{16}$$

The source voltage and current are denoted by V_S and I_S, whereas the proportional and integral gain are denoted by K_p and K_i. The PI controller outputs hysteresis controller reference current.

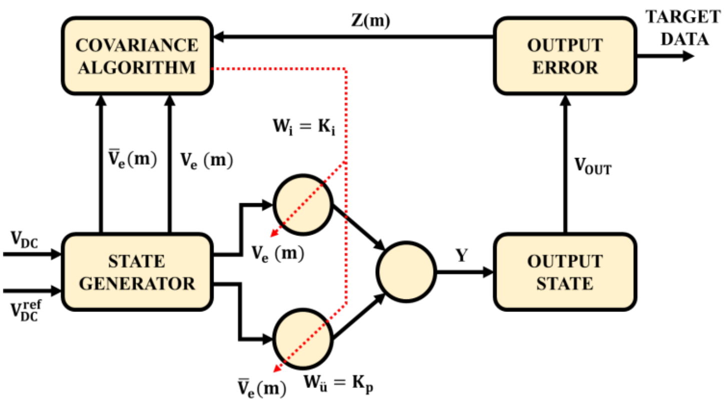

Figure 6. ANN based controller structure

2.3. Hysteresis controlled PWM circuit

Hysteresis PWM control uses inductor current feedback signals for exact outcomes. Instead of adding an inductor winding, the new hysteresis-regulated PWM circuit uses a simple RC network between the comparator and converter outputs. The RC integral circuit creates a triangle voltage from the comparator output when its AC component is added as the comparator input. Notably, converter input voltage does not affect switching frequency.

The controller's transfer process exhibits derivative characteristics, where the coefficient is directly proportional to the time constant of the RC integral circuit. At the switching frequency fs, if the impedance of the capacitor is lower compared to the resistance R2, the controller achieves improved performance.

$$\frac{1}{2\pi f_S C_1} \ll R_2 \tag{17}$$

The switching frequency is given as (18).

$$f_s = \frac{DV_{CP}}{V_H T_C} \tag{18}$$

The hysteresis voltage V_H, duty cycle (D), and time constant T_C are supplied.

3. RESULTS AND DISCUSSION

This research proposes a new charging technique for a battery-operated electric vehicle (BEV) with improved PFC. This technique comprises a bridgeless Landsman converter, ANN based PI controller in addition to hysteresis controller based PWM generator. The entire technique is simulated using MATLAB. The parameter specifications for the bridgeless Landsman converter are given in Table 1.

Current and voltage waveforms of an AC source are depicted in Figure 7. The input AC current first varies from +2.5 A to -2.5 A and then stabilizes between +2 A to -2 A. AC voltage waveforms are stable about 70 V. Figure 8 shows the input AC supply power waveform. The bridgeless Landsman converter receives 50 W to 70 W from 0.6 s. The voltage across capacitor C_1 and C_2 is given in Figures 9(a) and 9(b). The load current is shown in Figure 10(a), and the load voltage waveform is given in Figure 10(b). As illustrated in Figure 11, the proposed control approach using an ANN-based bridgeless Landsman converter achieves a unity power factor, thereby enabling efficient and rapid charging of electric vehicle (EV) batteries.

Table 1. Parameter specifications for the bridgeless Landsman converter

Parameters	Values
Power rating	$1\ kW$
Input AC voltage range (V_{AC})	180 to 270 V
Output DC voltage range (V_{DC})	270 to 330 V
L_{I1}, L_{I2}	$1\ mH$
L_{01}, L_{O2}	$3.7\ mH$
C_1, C_2	$47\ \mu F$
C_O	$570\ \mu F$

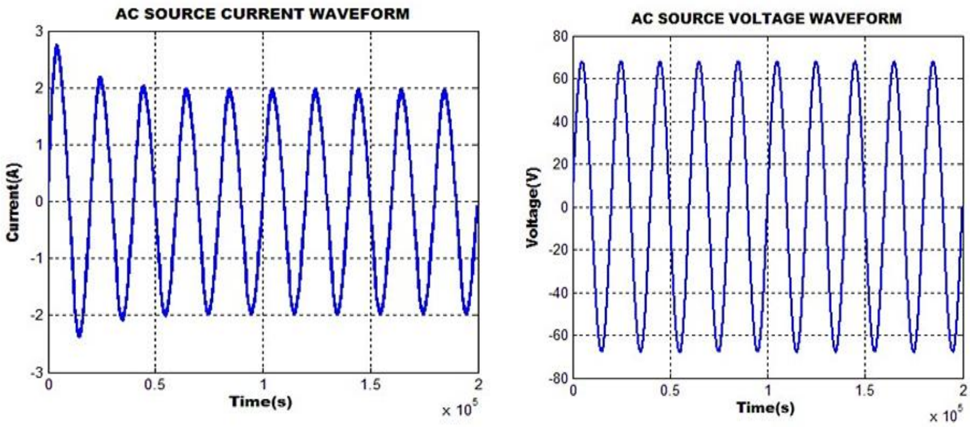

(a) (b)

Figure 7. Input AC source: (a) current waveform and (b) voltage waveform

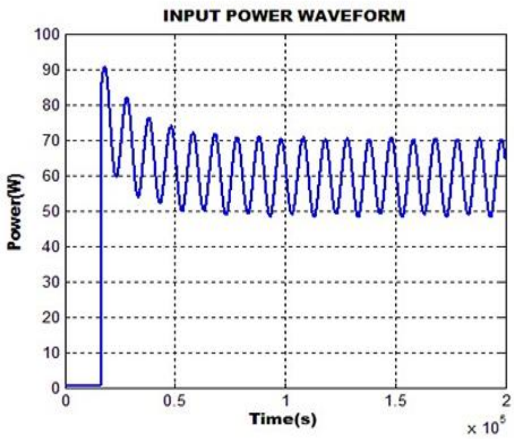

Figure 8. Input power waveform

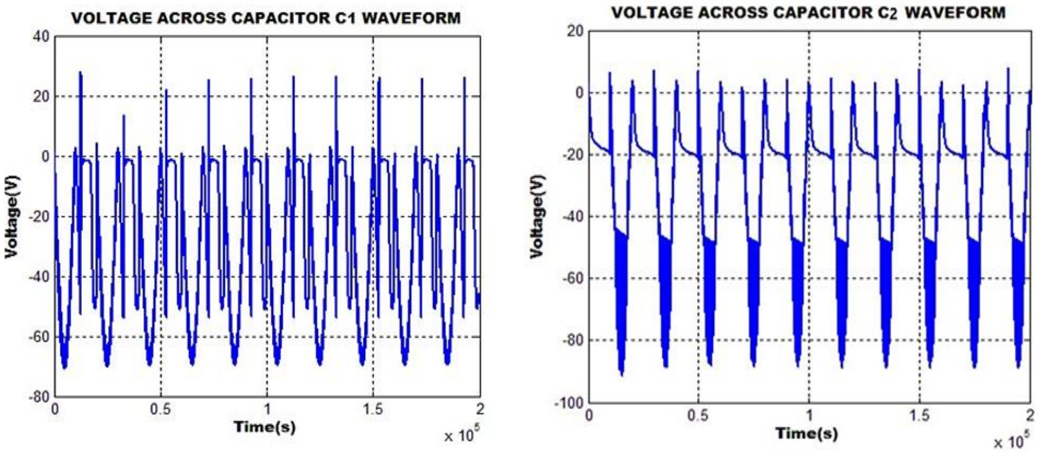

(a) (b)

Figure 9. Voltage waveforms across the capacitors: (a) voltage across capacitor C_1, and (b) voltage across capacitor C_2

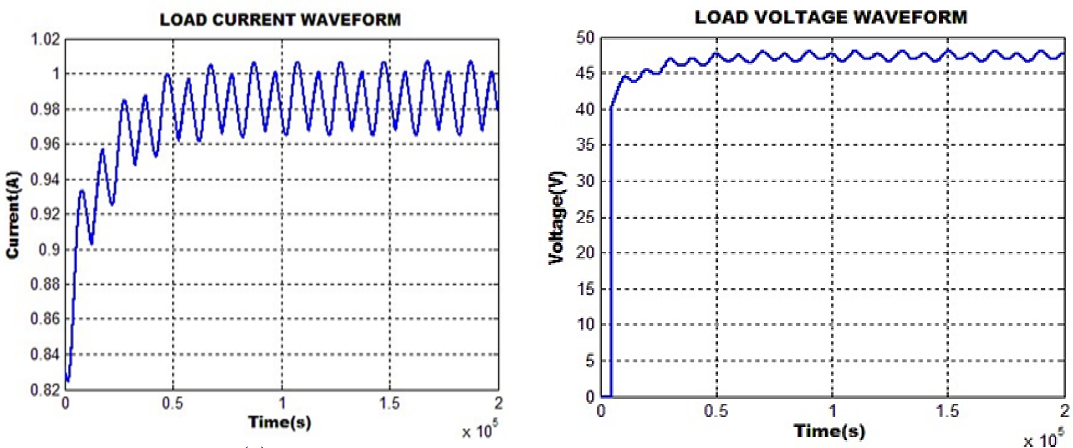

(a) (b)

Figure 10. Converter load waveforms: (a) load current and (b) load voltage

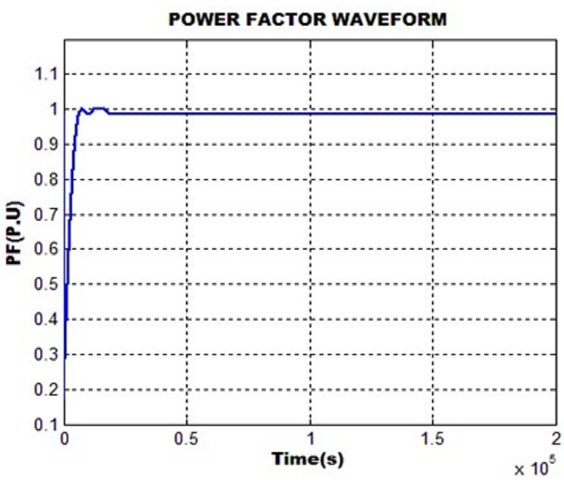

Figure 11. Power factor waveform

4. CONCLUSION

Electric vehicles (EVs) are gaining widespread adoption due to their numerous advantages, including advanced battery storage systems, low carbon emissions, and environmentally friendly operations. This study proposes a rapid and efficient EV battery charging system utilizing a BLC. The inclusion of inductors at both the input and output sides of the converter significantly reduces current ripples, ensuring stable and noiseless operation.

To enhance system performance, an artificial ANN-based PI controller is integrated, enabling quick estimation and precise management of the reference voltage. This hybrid control strategy improves prediction and classification processes, contributing to more reliable converter operation. Additionally, a hysteresis controller is implemented to accurately estimate the steady-state switching frequency, further optimizing the converter's performance. The proposed PFC technique is validated through MATLAB simulations, demonstrating its effectiveness in achieving fast and efficient EV battery charging. The results underscore the potential of the proposed approach to minimize power quality issues, enhance system efficiency, and support the rapid adoption of EV technology.

FUNDING INFORMATION

This research was supported by Koneru Lakshmaiah Education Foundation, SERB, DST (EEQ/2023/000744).

AUTHOR CONTRIBUTIONS STATEMENT

This journal uses the Contributor Roles Taxonomy (CRediT) to recognize individual author contributions, reduce authorship disputes, and facilitate collaboration.

Name of Author	C	M	So	Va	Fo	I	R	D	O	E	Vi	Su	P	Fu
Podila Purna Chandra Rao	✓	✓	✓	✓	✓	✓		✓	✓	✓			✓	
Radhakrishnan Anandhakumar		✓				✓		✓	✓	✓	✓	✓		
T. Vijay Muni	✓	✓	✓	✓		✓	✓		✓	✓	✓		✓	✓
L. Shanmukha Rao				✓	✓					✓		✓		

C : **C**onceptualization	I : **I**nvestigation	Vi : **Vi**sualization
M : **M**ethodology	R : **R**esources	Su : **Su**pervision
So : **So**ftware	D : **D**ata Curation	P : **P**roject administration
Va : **Va**lidation	O : Writing - **O**riginal Draft	Fu : **Fu**nding acquisition
Fo : **Fo**rmal analysis	E : Writing - Review & **E**diting	

CONFLICT OF INTEREST STATEMENT

Authors declare that they do not have any conflict of interest.

DATA AVAILABILITY

Data availability is not applicable to this paper as no new data were created or analyzed in this study.

REFERENCES

[1] R. Kushwaha and B. Singh, "Power factor improvement in modified bridgeless Landsman converter fed ev battery charger," *IEEE Transactions on Vehicular Technology*, vol. 68, no. 4, pp. 3325–3336, 2019, doi: 10.1109/TVT.2019.2897118.

[2] S. M. Shariff, M. S. Alam, F. Ahmad, Y. Rafat, M. S. J. Asghar, and S. Khan, "System design and realization of a solar-powered electric vehicle charging station," *IEEE Systems Journal*, vol. 14, no. 2, pp. 2748–2758, 2020, doi: 10.1109/JSYST.2019.2931880.

[3] A. Mallik, J. Lu, and A. Khaligh, "Sliding mode control of single-phase interleaved totem-pole PFC for electric vehicle onboard chargers," *IEEE Transactions on Vehicular Technology*, vol. 67, no. 9, pp. 8100–8109, 2018, doi: 10.1109/TVT.2018.2848238.

[4] S. G. Kumar, P. Muhilan, and M. S. Kumar, "Bridgeless Landsman converter for electric vehicle," *13th IEEE International Conference on Smart Grid, icSmartGrid 2025*, 2025, pp. 757–760, doi: 10.1109/ICSMARTGRID66138.2025.11071814.

[5] J. Liu, K. W. Chan, C. Y. Chung, N. H. L. Chan, M. Liu, and W. Xu, "Single-stage wireless-power-transfer resonant converter with boost bridgeless power-factor-correction rectifier," *IEEE Transactions on Industrial Electronics*, vol. 65, no. 3, pp. 2145–2155, 2018, doi: 10.1109/TIE.2017.2745471.

[6] T. V. Muni and S. V. N. L. Lalitha, “Implementation of control strategies for optimum utilization of solar photovoltaic systems with energy storage systems,” *International Journal of Renewable Energy Research*, vol. 10, no. 2, 2020.

[7] B. Chandrasekar *et al*., “Non-isolated high-gain triple port DC-DC buck-boost converter with positive output voltage for photovoltaic applications,” *IEEE Access*, vol. 8, pp. 113649–113666, 2020, doi: 10.1109/ACCESS.2020.3003192.

[8] Q. Huang, A. Q. Huang, R. Yu, P. Liu, and W. Yu, “High-efficiency and high-density single-phase dual-mode cascaded buck-boost multilevel transformerless PV inverter with GaN AC switches,” *IEEE Transactions on Power Electronics*, vol. 34, no. 8, pp. 7474–7488, 2019, doi: 10.1109/TPEL.2018.2878586.

[9] J. C. D. S. De Morais, J. L. D. S. De Morais, and R. Gules, “Photovoltaic AC module based on a cuk converter with a switched-inductor structure,” *IEEE Transactions on Industrial Electronics*, vol. 66, no. 5, pp. 3881–3890, 2019, doi: 10.1109/TIE.2018.2856202.

[10] S. Kollati, D. R. Kishore, D. B. Sai, K. A. Danie, and P. S. Koushik, “Fuzzy MPPT controlled Landsman converter for grid tied PMBLDC based water pumping system,” in *2024 1st International Conference on Innovative Sustainable Technologies for Energy, Mechatronics, and Smart Systems (ISTEMS)*, Dehradun, India, 2024, pp. 1–6, doi: 10.1109/ISTEMS60181.2024.10560204.

[11] P. K. Inampudi, C. Perumal, V. R. Guntreddi, and T. V. Muni, “A novel DC-DC boost converter with coupled inductors for high gain and smooth switching,” *Journal of Advanced Research in Applied Sciences and Engineering Technology*, vol. 48, no. 2, pp. 92–104, 2025, doi: 10.37934/araset.48.2.92104.

[12] N. Kalaiarasi and R. M. Abdullah, “Power factor enhancement using a modified bridgeless Landsman converter driven EV battery charger,” *SAE Technical Papers*, 2023, doi: 10.4271/2023-28-0098.

[13] S. Padmanaban, N. Priyadarshi, M. S. Bhaskar, J. B. Holm-Nielsen, E. Hossain, and F. Azam, “A hybrid photovoltaic-fuel cell for grid integration with jaya-based maximum power point tracking: experimental performance evaluation,” *IEEE Access*, vol. 7, pp. 82978–82990, 2019, doi: 10.1109/ACCESS.2019.2924264.

[14] P. Inampudi, P. Chandrasekar, and T. V. Muni, “Evaluating a novel bidirectional soft-switching DC-DC converter for electric vehicles,” *International Journal of Applied Power Engineering*, vol. 13, no. 4, pp. 825–834, 2024, doi: 10.11591/ijape.v13.i4.pp825-834.

[15] K. S. Tey, S. Mekhilef, M. Seyedmahmoudian, B. Horan, A. T. Oo, and A. Stojcevski, “Improved differential evolution-based MPPT algorithm using SEPIC for PV systems under partial shading conditions and load variation,” *IEEE Transactions on Industrial Informatics*, vol. 14, no. 10, pp. 4322–4333, 2018, doi: 10.1109/TII.2018.2793210.

[16] T. V. Muni, S. V. N. L. Lalitha, B. R. Reddy, T. S. Prasad, and K. S. Mahesh, “Power management system in PV systems with dual battery,” *International Journal of Applied Engineering Research*, vol. 12, no. 1, pp. 523–529, 2017.

[17] K. Baig, K. P. Raj, G. G. R. Sekhar, T. V. Muni, and M. K. Kumar, “Power quality enchancement with active power control,” *Journal of Critical Reviews*, vol. 7, no. 9, pp. 739–741, 2020, doi: 10.31838/jcr.07.09.143.

[18] Z. Moradi-Shahrbabak and A. Tabesh, “Effects of front-end converter and DC-link of a utility-scale PV energy system on dynamic stability of a power system,” *IEEE Transactions on Industrial Electronics*, vol. 65, no. 1, pp. 403–411, 2018, doi: 10.1109/TIE.2017.2721902.

[19] B. T. Karim, A. Allali, H. M. Boulouiha, and M. Denai, “Voltage profile and power quality improvement using multicell dynamic voltage restorer,” *International Journal of Power Electronics and Drive Systems (IJPEDS)*, vol. 13, no. 4, pp. 2216–2225, 2022, doi: 10.11591/ijpeds.v13.i4.pp2216-2225.

[20] K. Nathan, S. Ghosh, Y. Siwakoti, and T. Long, “A new DC-DC converter for photovoltaic systems: coupled-inductors combined cuk-sepic converter,” *IEEE Transactions on Energy Conversion*, vol. 34, no. 1, pp. 191–201, 2019, doi: 10.1109/TEC.2018.2876454.

[21] R. Kushwaha and B. Singh, “Interleaved Landsman converter fed EV battery charger with power factor correction,” in *2018 IEEE 8th Power India International Conference (PIICON)*, 2018, pp. 1–6, doi: 10.1109/POWERI.2018.8704418.

[22] R. Garrido and A. Díaz, “Cascade closed-loop control of solar trackers applied to HCPV systems,” *Renewable Energy*, vol. 97, pp. 689–696, 2016, doi: 10.1016/j.renene.2016.06.022.

[23] S. Jadhav, N. Devdas, S. Nisar, and V. Bajpai, “Bidirectional DC-DC converter in solar PV system for battery charging application,” in *2018 International Conference on Smart City and Emerging Technology (ICSCET)*, Mumbai, India, 2018, pp. 1–4, doi: 10.1109/ICSCET.2018.8537391

[24] K. Nisha and R. Beniwal, “Comparison of efficiency of various DC-DC converters connected to solar photovoltaic module,” *Environmental Science and Pollution Research*, vol. 30, no. 30, pp. 75720–75734, 2023, doi: 10.1007/s11356-023-27761-0.

[25] W. Zhifu, W. Yupu, and R. Yinan, “Design of closed-loop control system for a bidirectional full bridge DC/DC converter,” *Applied Energy*, vol. 194, pp. 617–625, 2017, doi: 10.1016/j.apenergy.2016.11.113.

[26] L. Bouselham, M. Hajji, B. Hajji, and H. Bouali, “A new MPPT-based ANN for photovoltaic system under partial shading conditions,” *Energy Procedia*, vol. 111, pp. 924–933, 2017, doi: 10.1016/j.egypro.2017.03.255.

BIOGRAPHIES OF AUTHORS

Podila Purna Chandra Rao completed B.Tech. and M.Tech. from JNT University, Andhra Pradesh. He is pursuing Ph.D. at Annamalai University. His area of interest is power electronic converters and electric vehicles. He can be contacted at email: purnachandrarao.phd@gmail.com.

Dr. Radhakrishnan Anandhakumar is working as an assistant professor in the Department of Electrical Engineering, Faculty of Engineering and Technology, Annamalai University, Annamalai Nagar, Tamil Nadu, India. His area of interest includes optimization techniques in the power systems and power system reliability. He can be contacted at email: anand_r1979@yahoo.com.

T. Vijay Muni is an assistant professor and researcher with more than 14 years of experience in the Department of Electrical and Electronics Engineering at K L Deemed to be University. He received his B.Tech. degree in electrical and electronics engineering from JNTU Hyderabad, M.Tech. degree in power and industrial drives from JNTUK, Kakinada, and doctoral degree from K L Deemed to be University. He has authored 6 textbooks on electrical discipline. He has published over 61 Scopus-indexed articles, 15 Web of Science-indexed articles, and over 15 articles in peer-reviewed journals, and has also published 6 patents with two grants. His areas of research include power electronic converters, energy management systems, control of electric power grids, renewable energy systems, and microgrid. He is an active senior member of IEEE. He can be contacted at email: vijaymuni1986@gmail.com.

Dr. L. Shanmukha Rao is a research co-guide and professor in the Department of Electrical and Electronics Engineering, Kallam Haranadhareddy Institute of Technology, Chowdavaram, Guntur, Andhra Pradesh, India. His area of interest includes FACTS devices, power quality, deregulated power systems, and renewable energy resources. He can be contacted at email: lsrlingineni@yahoo.co.in.